Magazine of Civil Engineering

journal homepage: http://engstroy.spbstu.ru/

ISSN 2712-8172

Research article

UDC 691.88

DOI: 10.34910/MCE.112.2

Bearing capacity of riveted connections of mineral wool sandwich panels

A. Galyamichev [a], ***E. Gerasimova*** [b] ✉, ***D. Egorov*** [a], ***D. Serdjuks*** [c], ***A.M. Grossman*** [a], ***D.A. Lysenko*** [a]

[a] *Peter the Great St. Petersburg Polytechnic University, St. Petersburg, Russia*

[b] *NIUPC, Mezhregional'nyj institut okonnyh i fasadnyh konstrukcij, St. Petersburg, Russia*

[c] *Riga Technical University, Riga, Latvia*

✉ *katyageras17@gmail.com*

Keywords: bearing capacity, sandwich structures, facades, dynamic loads, pull-out strength, connectors

Abstract. The article presents a study on the pulling-out bearing capacity of the connection between a curtain wall system and an outer sheet of a wall sandwich panel with a mineral wool core realized through blind rivets. An experimental study was carried out on samples of sandwich panels with various parameters of fastening in order to assess the influence of the considered factors on the value of bearing capacity. Results obtained for the studied type of sandwich panel allowed us to determine the minimum permissible edge distance for a blind rivet in order to prevent delamination of the outer sheet as well as the influence of the end profile installation and cyclic load action on the bearing capacity of the joint. Experimental results showed that the edge distance of 75 mm or more does not affect the bearing capacity of the joint. The pulling-out bearing capacity of a blind rivet with a diameter of 4.8 mm was determined for both single and cyclic load actions. The presence of an additional stiffening element such as end face profile contributed to an increase of this value. Recommended scheme for the installation of the fastening elements was proposed based on dependencies obtained during the experimental investigation.

Acknowledgement: The research group would like to thank Prof. Dr.-Ing. Jörg Lange, TU Darmstadt, Germany, for his assistance and contributions. Furthermore, we would like to thank company ISOPAN for providing the samples of sandwich panels, and companies Alternativa and U-kon for supplying with the samples of curtain wall systems.

Citation: Galyamichev, A., Gerasimova, E., Egorov, D., Serdjuks, D., Grossman, A.M., Lysenko, D.A. Bearing capacity of riveted connections of mineral wool sandwich panels. Magazine of Civil Engineering. 2022. 112(4). Article No. 11202. DOI: 10.34910/MCE.112.2

1. Introduction

Nowadays in construction practice three-layer sandwich panels are often used as enclosing structures in buildings and facilities for various purposes because of their weight, cost, and structural characteristics. Different cladding types such as aluminum composite panels, fiber cement boards, or high-pressure laminate (HPL) panels can be applied for covering the external walls made of three-layer sandwich panels on new construction sites (Figures 1 and 2) as well as for existing buildings under reconstruction (Figure 3).

Figure 1. Platov Airport, Rostov-on-Don (Russia).

Figure 2. Historical park "Russia – my history", Volgograd (Russia).

Figure 3. Shopping mall «MEGA Khimki», Moscow (Russia).

Several fastening options exist depending on the structural scheme of a cladding system attachment to the external sandwich panel:

- Fastening to bearing structures situated behind a sandwich panel (through);
- Fastening to an external framework;
- Fastening to an outer metal sheet.

This paper presents a study on the fastening to the outer steel sheet of the sandwich panel with mineral wool insulation core. One of the main reasons of failure when the system no longer fulfills the Ultimate Limit State conditions is the delamination of the sandwich panel (Figure 4) [1]. Delamination occurs under a variety of dynamic and quasi-static load conditions [2], therefore it should be carefully revised when designing an enclosing structure.

Within the framework of this study, the delamination of sandwich panels with the mineral wool core is analyzed. Such a phenomenon was already observed among other failure modes for sandwich panels with other types of core, such as multi-layered aluminum foam core and multi-layered hybrid aluminum foam / ultra-high-molecular-weight polyethylene (UHMWPE) laminate core in [3]. Article [4] presents an overview and failure maps on the dependencies of the critical failure modes including the delamination on the structural parameters and load/support combinations for sandwich panels with polyurethane (PUR) core. The flexural properties, collapse modes, and crush characteristics of different types of composite panels are described in [5] on the basis of series of flexural tests. The panels were subjected to both mechanical and thermal actions. Polyurethane (PUR) and polyvinylchloride (PVC) core sandwich panels subjected to tension, compression, and shear loading were tested and modeled using the Finite Element Method in [6] taking into account non-linear behavior of the foam core and skin-core cohesive interaction. Foam-core sandwich composites subjected to low-velocity impact are studied in [7]. The study [8] is dedicated to the detection of delamination in composite structures including the ones with PUR core under free vibration. The peculiarity of low-velocity impact response of synthetic foam core panels is defined in [9], and high-velocity impact is simulated in [10].

Dynamic interfacial debonding in sandwich panels was studied in [11], where the authors applied a nonlinear dynamic analytical approach in order to investigate the structural behavior of panels and their failure mechanism. As the character of loading significantly influences the structural response, it is necessary to take into account load characteristics at both the experimental and numerical modeling stages. Article [12] demonstrates experimental and numerical results of the research on damage sequence including debonding and delamination of honeycomb sandwich panels subjected to bending. The effect of shear loading on the mechanical response of a Y-frame core sandwich panel was investigated in [13]. According to [13], delamination failure was the dominant failure mode for the considered type of panels.

The low-velocity impact on the sandwich panel with honeycomb core is studied in [14]. The article contains a comparison of the results obtained for various damage modes. The mechanical behavior of foam-filled corrugated core panels in lateral compression is discussed in the study [15]. Experiments identified localized delamination as well as debonding between layers.

Recent researches in the field of innovative materials and technologies offer a vision for the development of products with enhanced characteristics. For panel strengthening and improvement of its structural performance by means of increased stiffness, the panels can be reinforced with special glass fiber reinforced polymer ribs [16]. Another potential solution for obtaining better properties such as resistance to delamination of sandwich panels is the use of 3D fabrics made of glass fiber [17].

High-quality bonding of core and skins is one of the key factors for providing overall stiffness and structural strength [18]. Different methodologies can be applied for modeling the cohesive zone in sandwich panels [19], [20]. Paper [21] proposes a calculation methodology for determining the critical energy release rate for interfacial delamination.

Experimental investigations of the load-bearing capacity taking into account face sheet and foam core interaction within a sandwich panel are presented in [22]. The analysis provided in the research leads to the development of a consistent model, which proposes modifications to the current design and calculation methodologies.

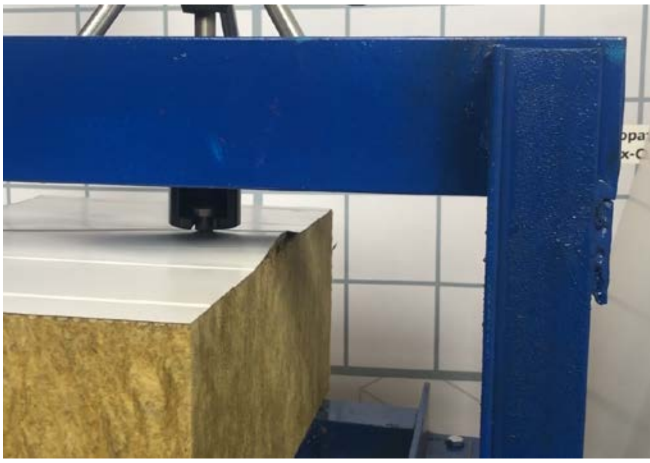

Figure 4. Delamination of the outer sheet of wall sandwich panel.

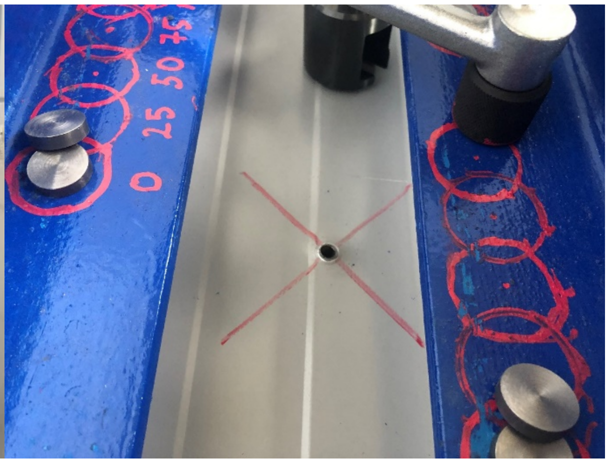

Figure 5. Pulling of a rivet from steel sheet.

The aim of the study was to determine the value of the bearing capacity of the connection between the rivet and an outer sheet of the sandwich panel, the influence of the installation of an end face profile and the cyclic load on this value, and the critical edge distance in order to prevent delamination. The research aimed at the characterization of the principal limiting factors and test approach for the structural solution where fastening was made to an outer metal sheet of a sandwich panel. The study addressed the following tasks:

- Performing an experimental study to determine the minimum allowable distance from the edge of a sandwich panel for installing a blind rivet;
- Determining the bearing capacity of the fastening by a group of blind rivets under the action of pulling force;
- Determining the bearing capacity of the fastening by a group of blind rivets under the combined action of pulling and shear forces;
- Determining the effect of shear forces on joint performance.

2. Methods

The characteristic feature of the study is the usage of the special equipment, which does not directly affect the tested panel sheet (Figure 6). Panel's fastening to the test bench is performed on the lower side of the panel while pulling force is applied to the rivet installed on the upper metal sheet. The experimental setup shown in Figures 6 and 7 was used for the tests described in sections 2.1 to 2.3. The experimental setup for the tests described in section 2.4 is shown in Figure 21.

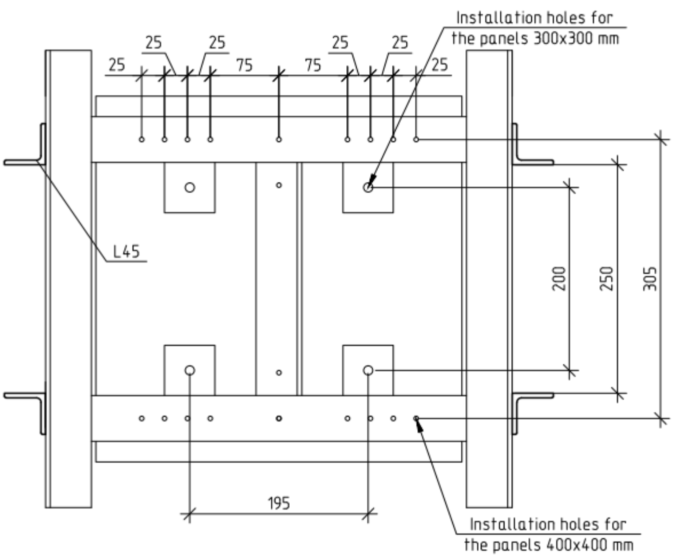

Figure 6. Location of sandwich panel fastening points on the test setup, top view.

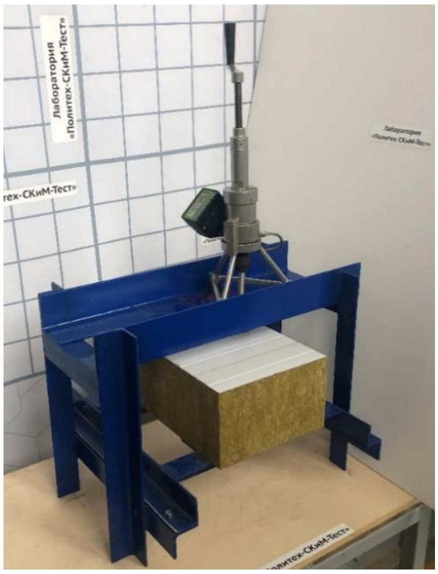

Figure 7. Test setup.

In this study, tests were carried out on a blind rivet of the structure shown in Figures 8 and 9. The designations shown in Figure 8 have the following meaning: D is a rivet body diameter; L is a rivet length; D_k is rivet head diameter; K is a rivet body height; G is a grip range; F is work hole diameter. The designations shown in Figure 9 refer to the parts of the rivet body: 1 is a rivet body end; 2 is a rivet head; 3 is a cylindrical part of the rivet; 4 is an inner space of the rivet body.

In this study, the rivets had the rivet body diameter D of 4.8 mm, the rivet head diameter D_k of 14 mm, and the rivet length L of 21 mm.

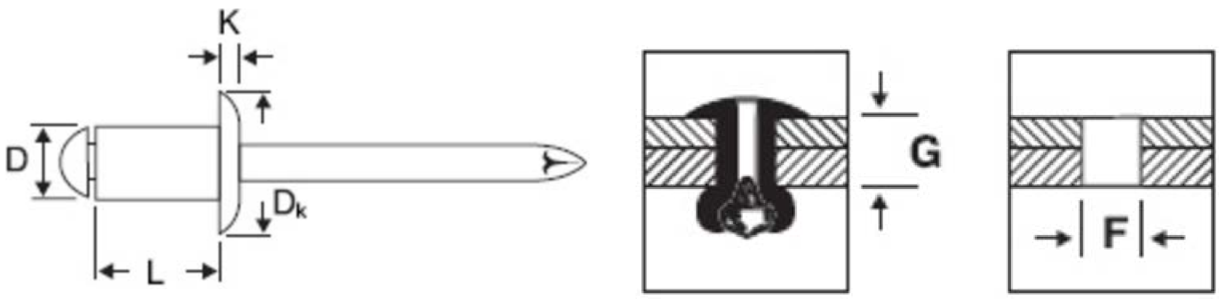

Figure 8. Blind rivet.

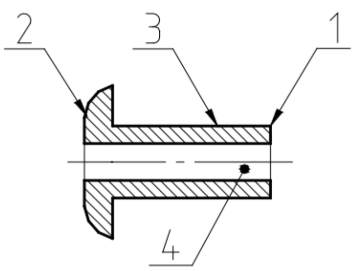

Figure 9. Rivet body.

The rivets were made of steel type 08X18H10 in Russian classification, analogous to AISI 304 (USA), 1.4301 (European Union). The mechanical properties of steel are shown in Table 1.

Table 1. Strength of steel of rivets.

Characteristic value		Design value	
Yield strength f_y, MPa	Ultimate strength f_u, MPa	Yield strength f_y, MPa	Shear strength v_c, MPa
185	510	175	100

The sandwich panels consisted of two metal sheets with a nominal thickness of 0.5 mm bonded to each side of a mineral wool core with a thickness of 150 mm. The material of metal sheets is galvanized steel 08ps in Russian classification with a nominal yield strength of 230 MPa. The nominal weight of the zinc layer declared by the manufacturer was 140 g/m^2.

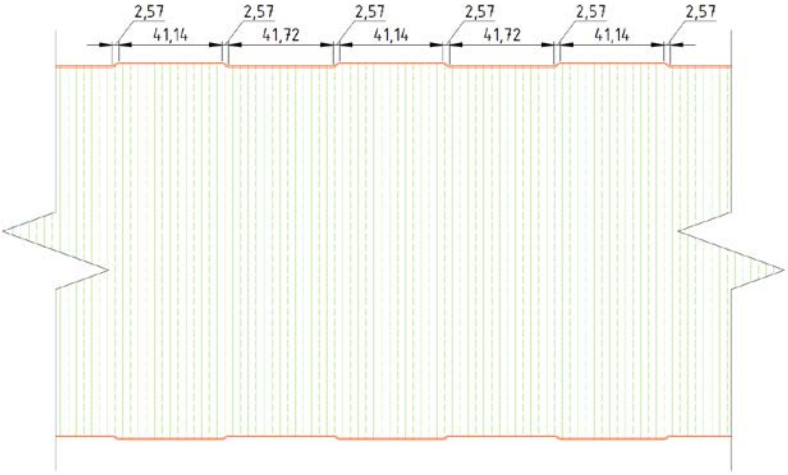

Figure 10. Profile of the sandwich panel.

The mineral wool core had the following nominal characteristics according to the technical manual provided by the manufacturer:

- Average density: 100 kg/m^3;
- Compression strength: 0.06 MPa (at 10% deformation);
- Tensile strength: 0.04 MPa according to EN 826:2013;
- Shear strength: 0.05 MPa according to EN 826:2013.

The values of strength were measured transverse the fibers.

The core was glued to the metal sheets by two-component polyurethane adhesive on the basis of isocyanate and polyol.

In sections 2.1 to 2.3 sandwich panels were attached to the lower level of the test bench with the creation of a fastening, which significantly exceeds the bearing capacity of the considered joint connection. The location of sandwich panel fastening points on the test bench is shown in Figure 6.

A test sleeve (Figure 11) was riveted to the outer sheet of the panel at a predetermined edge distance. The rivet was pulled out by means of an equipped tensile force measurer (PSO-20MG4A AD, Figure 12) using the test sleeve. Tensile force measurer was mounted on the upper level of the test bench (without contact with the surface of the sandwich panel). The speed of pulling out varied from 7 to 13 mm/min. The tensile force measurer had a speed indicator. Pulling out lasted until the loss of the bearing capacity of the joint (between a rivet and a sandwich panel) or directly a sandwich panel. The failure was determined by analysis of the displacement-load graphs, as well as visually and considering the appearance of characteristic sounds.

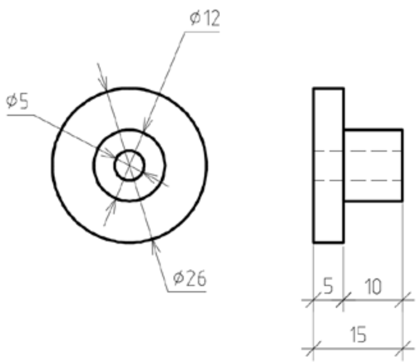

Figure 11. Test sleeve

Figure 12. Tensile force measurer PSO-20MG4A AD

2.1. Test procedure for the panels with various values of the edge distance

Edge distance was defined as the distance from the center of the rivet to the edge of the sandwich panel. Five configurations of sandwich panels with different edge distances were subjected to testing (Table 2).

Table 2. Configurations of sandwich panel samples.

Size of the panel	Edge distance, mm
400×400 mm (Figure 13, left)	200
400×250 mm (Figure 13, right)	50
400×400 mm	75
400×300 mm	100
400×350 mm	150

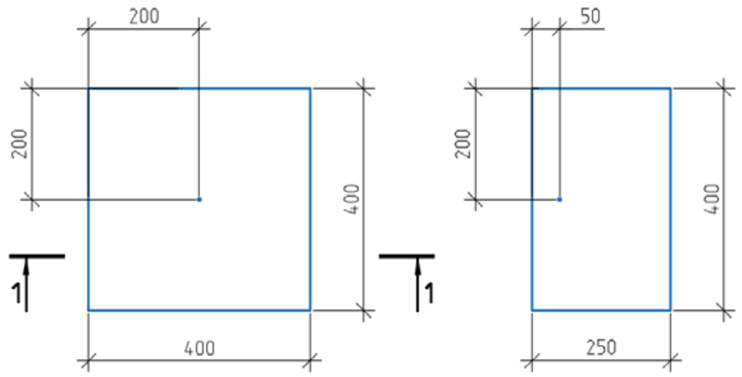

Figure 13. Test samples of sandwich panels

2.2. Test procedure for the panels with installed end face profile

Sandwich panels with dimensions of 400×400 mm and an edge distance of 50 mm in two different variations were subjected to testing (Figures 14 and 15).

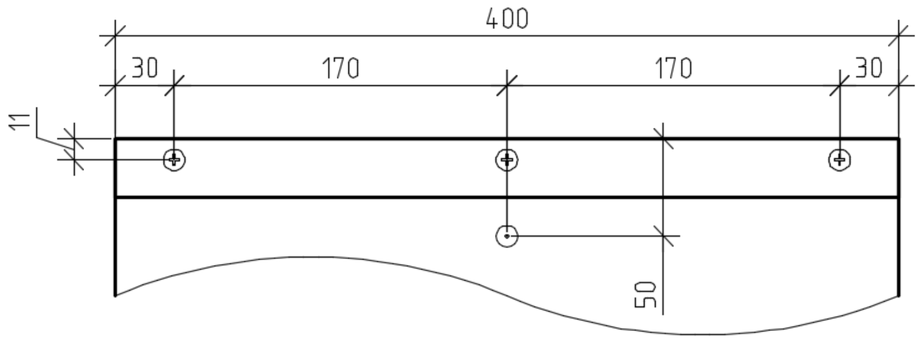

Figure 14. Coaxial scheme of placement of self-tapping screws.

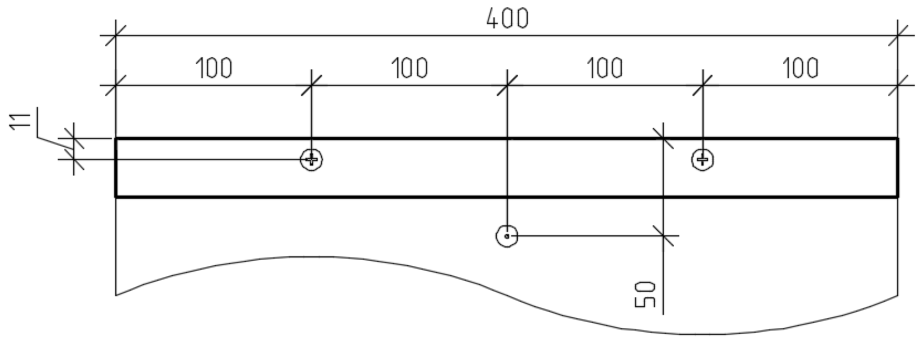

Figure 15. Span scheme of placement of self-tapping screws.

A cold-formed profile made of galvanized steel sheet was attached by self-tapping screws. In this study, the profile shown in Figure 16 had the following dimensions: a = 150 mm, b = 30 mm, t = 0.5 mm.

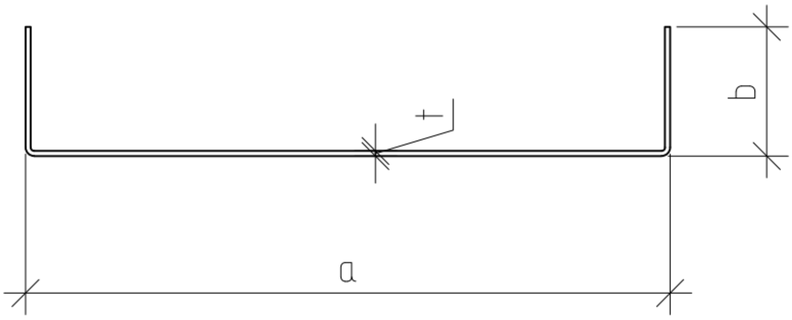

Figure 16. Drawing of the profile.

Steel self-tapping screws had a diameter of 4.2 mm and length of 19 mm in accordance with DIN 968.

Figure 17. Coaxial and span fastening schemes.

Figure 18. Edge distance of 50 mm in the coaxial scheme.

2.3. Test procedure for the panels under cyclic load action

Cyclic loading imitated peak wind load applied to the sandwich panel. The duration of single load application was set to 3 seconds in accordance with ASCE 7-05 regulations. Two types of cycles were considered: non-uniform and uniform (Table 3).

Samples with dimensions of 400×400 mm (20 units) and an edge distance of 200 mm were subjected to testing. On one side of the panel, test sleeves were fixed to the test specimen by blind rivets, and, on the other side, a T-shaped embedded plate with a width of 80 mm was attached by self-tapping screws with the creation of a fastening, significantly exceeding the bearing capacity of the studied joint connection.

Obtained samples were installed in a universal machine for tensile and compression tests (Zwick/Roell Z100). A concentrated, successively alternating load was applied to the test sleeve. The test speed ranged from 7 to 13 mm/min.

During the test, both uniform and non-uniform cycles were applied.

The value of the load was chosen in order to maintain the bearing capacity for at least 365 non-uniform and 485 uniform cycles.

According to the Russian Set of Rules 20.13330.2016 “Loads and actions”, as a result of peak wind exposure, a non-uniform cycle is characteristic for corner zones of buildings while a uniform cycle is characteristic for ordinary zones.

Table 3. Characteristics of uniform and non-uniform cycles

<table>
<tr><th>Non-uniform cycle</th><th>Uniform cycle</th></tr>
<tr><td colspan="2">Concentrated pulling force</td></tr>
<tr><td colspan="2">P_{-}</td></tr>
<tr><td colspan="2">Concentrated pressing force</td></tr>
<tr><td>$P_{+} = \frac{P_{-} \cdot 1.2}{2.2} = 0.55 \cdot P_{-}$</td><td>$P_{+} = P_{-}$</td></tr>
<tr><td>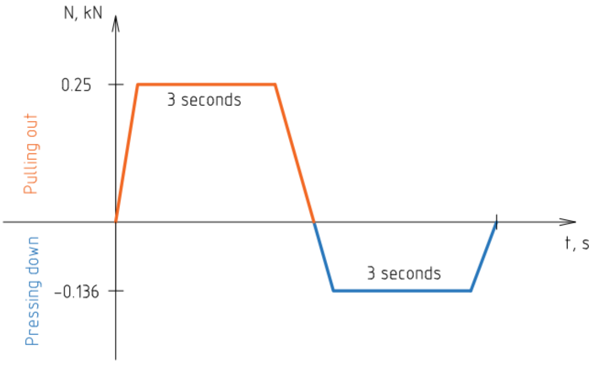
</td><td>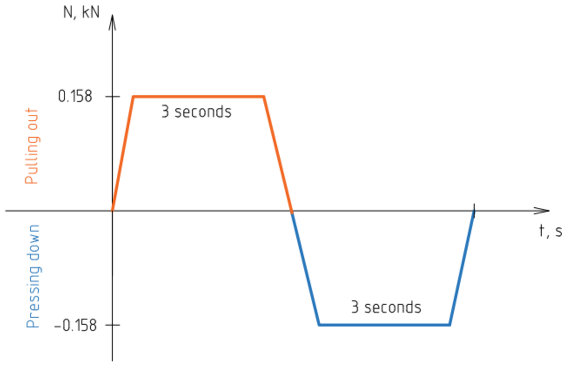
</td></tr>
<tr><td>Example of a non-uniform cycle (+0.25 kN / -0.136 kN)</td><td>Example of a uniform cycle (+0.158 kN / -0.158 kN)</td></tr>
</table>

$$c_{p\ corner} = -2.2; c_{p\ ordinary} = 1.2; \frac{c_{p\ corner}}{c_{p\ ordinary}} = -1.83$$

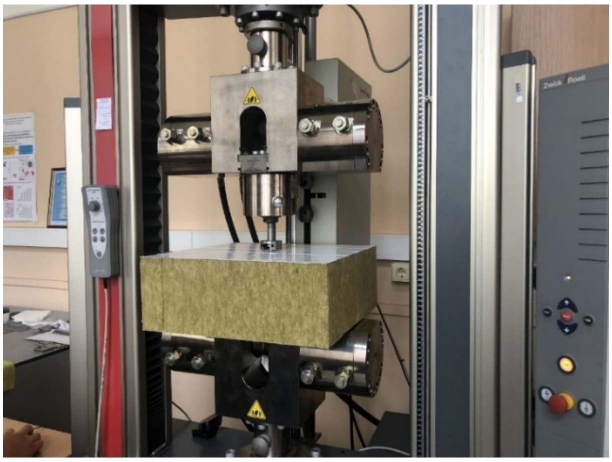

Figure 19. Test sample installed in Zwick/Roell Z100

2.4. Test procedure for a group of rivets subjected to pulling

The tests were performed on a full-sized sample of a sandwich panel under conditions of a complex stress state, which correspond to the actual operation of the system. The sandwich panel was clamped to the bearing base at four points. Steel clamps retained the panel through distribution pads. The profile shown in Figure 20 was riveted to the outer sheet of the sandwich panel in accordance with the schemes shown in Figures 24 to 28.

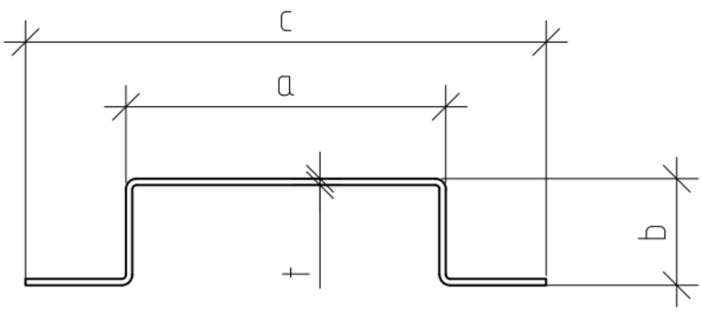

Figure 20. Cross-section of the profile used in the test

Figure 21. Test setup for the study of a cyclic load

The test consisted of two variations:

1. A constant load of 0.3 kN was applied to the sample in the plane of the facade structure while a load applied out of the plane (simulating the wind effect) was sequentially increased by means of contracting jack in order to determine the critical value of the above-indicated force.

2. The test procedure was set similarly to clause 1, but without applying a constant load in the plane of the facade structure.

The magnitude of the load and the type of failure at which the loss of the bearing capacity occurred were recorded.

The test sample was a fragment of a wall sandwich panel with an installation width of 1190 mm and length of 1000 mm. The sandwich panel was fixed to the base at four points by steel clamps with distribution pads.

Test schemes are shown in Figure 22 and Figure 23:

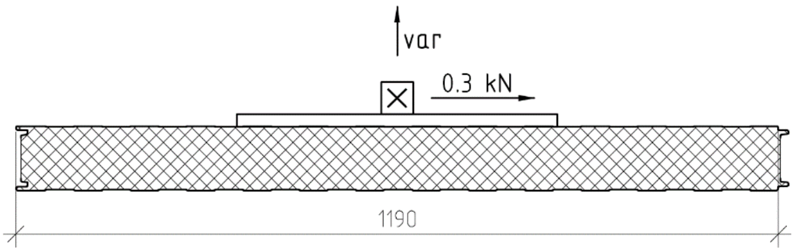

Figure 22. Scheme with the combined action of shear force and pulling force (modification 1).

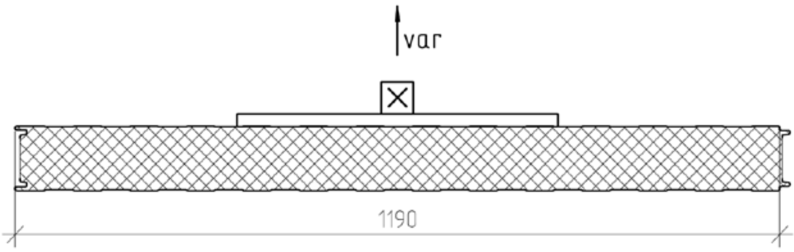

Figure 23. Scheme with the action of pulling force (modification 2).

Several test schemes (Figures 24 – 28) were tested in order to evaluate the influence of fastening parameters on the occurrence of delamination.

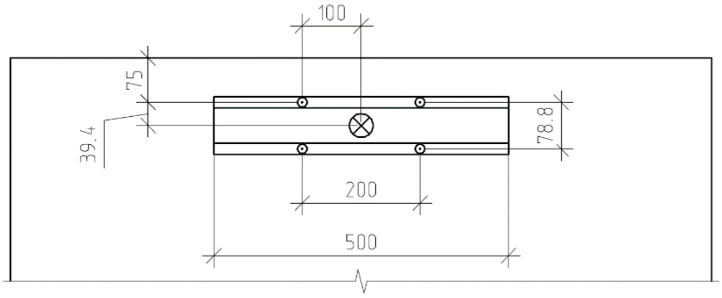

Figure 24. First scheme option.

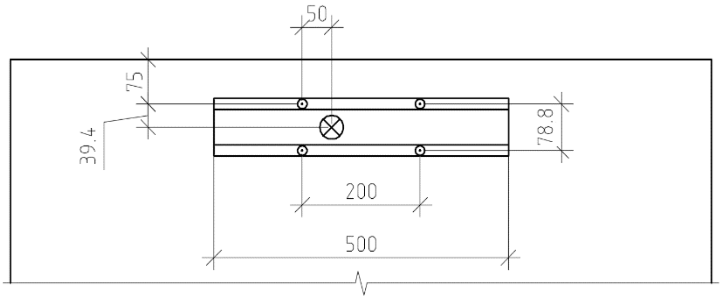

Figure 25. Second scheme option.

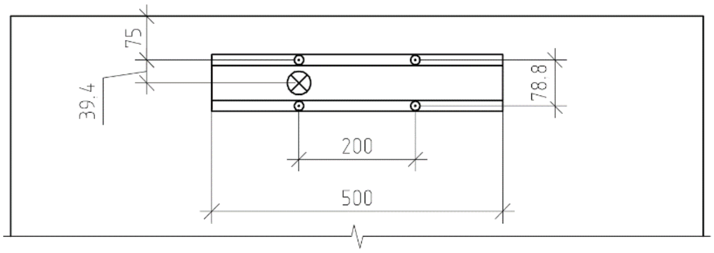

Figure 26. Third scheme option.

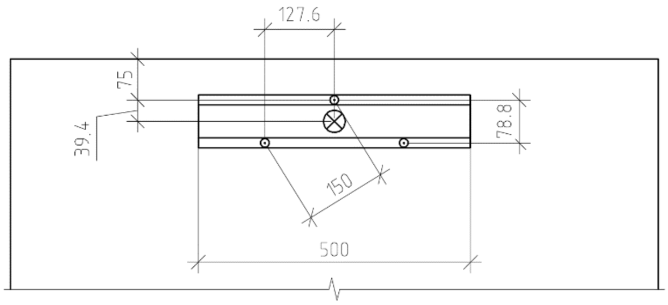

Figure 27. Forth scheme option (coaxial).

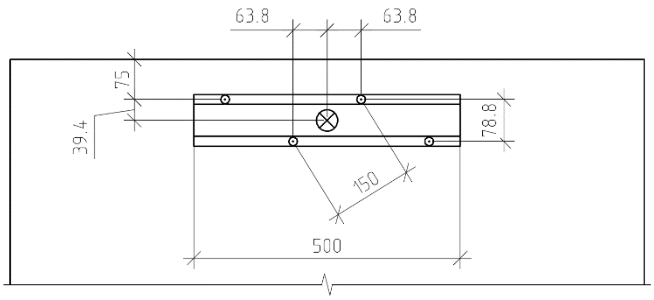

Figure 28. Fifth scheme option (span).

3. Results and Discussion

Depending on the method of load application, characteristics of the bearing capacity of the joint were determined either based on unit values of the destructive load or based on load values corresponding to the end of the elastic deformation zone.

One or two extreme values were excluded from the series of unit results if their absolute value and (or) the nature of failure sharply differed from the series of values.

The average load value, the standard deviation of the unit load values, and the coefficient of variation were calculated using formulas (1), (2), and (3) for the series of unit test results N_i.

Average load value:

$$N_{average} = \frac{\sum_{i=1}^{n} N_i}{n} \tag{1}$$

Standard deviation of the unit load values:

$$S = \sqrt{\frac{\sum_{i=1}^{n} (N_i - N)^2}{n-1}} \tag{2}$$

Coefficient of variation:

$$v = \frac{S}{N} \tag{3}$$

Allowable load (without safety factor):

$$F_n = \frac{N(1-tv)}{\gamma_n} \tag{4}$$

where t is the Student's coefficient of the confidence interval of 0.95. For performed 59 tests (n = 59):

t = 2.00099

γ_n is coefficient of working conditions, taken equal to 1.1, since the fastenings are installed in the laboratory;

N_i is unit load value in series of test results, kN;

n is the number of results within the series.

If the excluded from series results N_i went beyond the limits equal to $N \pm 3S$, they were finally discarded. If the excluded results N_i did not go beyond the specified limits, then the values of N, $\underline{S}$ and v were recalculated according to the results of the entire series of unit tests.

3.1. Pulling test

The test according to chapter 2.1 was carried out on 15 samples for each considered value of the edge distance.

Table 4. Summarized test results.

Edge distance, mm	Average value of pulling force, kN	Character of a fracture
50	0.570	delamination (87% of the total amount of samples)
75	0.625	pulling (100% of the total amount of samples)
100	0.615	pulling (100% of the total amount of samples)
150	0.613	pulling (100% of the total amount of samples)
200	0.591	pulling (100% of the total amount of samples)

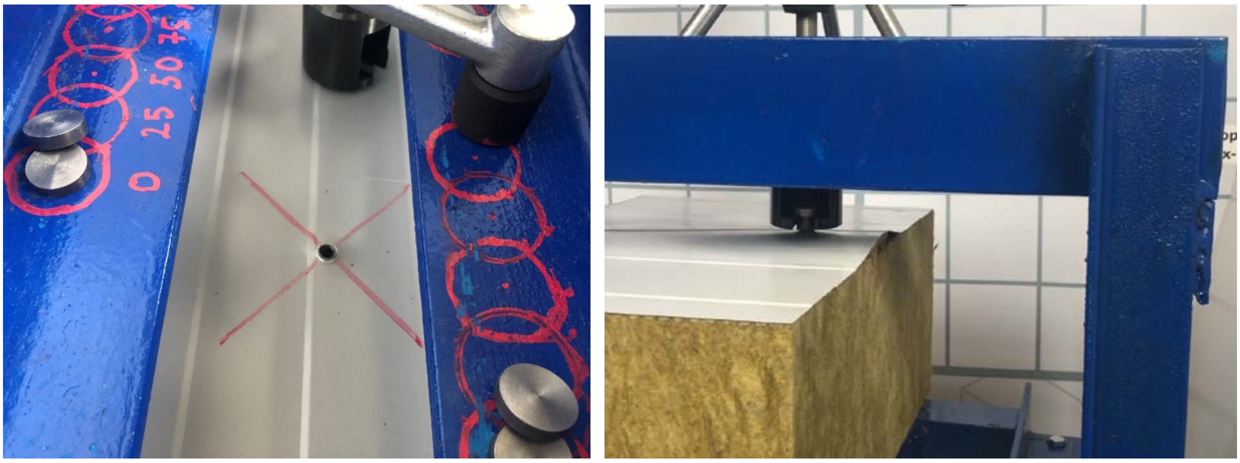

Figure 29. Left – fracture by pulling out of the outer sheet of the sandwich panel; right – fracture by delamination of the outer sheet of the sandwich panel.

Due to the uniform nature of the fracture of the samples (except delaminated panels) and the absence of a relationship between edge distance and the magnitude of the pulling force, obtained values were combined in order to evaluate the bearing capacity of rivet fastening of curtain facade system to wall sandwich panel.

Average load value:

$$N_{average} = \frac{36.13}{59} = 0.612kN$$

Standard deviation of the unit load values:

$$S = \sqrt{\frac{0.11687}{59-1}} = 0.045kN$$

Coefficient of variation:

$$v = \frac{0.045}{0.612} = 0.073$$

Bearing capacity (without safety factor) of the connection between a blind rivet with a diameter of 4.8 mm and the outer sheet of a sandwich panel with a thickness of 0.5 mm under a single loading of the sample:

$$F_n = \frac{0.612 \cdot (1 - 2.00099 \cdot 0.073)}{1.1} = 0.475kN$$

When the distance from the edge of the sandwich panel to the axis of the installed blind rivet (edge distance) was equal to 50 mm, destruction due to delamination occurred in 87% of the samples.

When the edge distance was equal to 75 mm and more from the range of considered values, pull-out failure occurred in 100% of the samples.

3.2. Pulling test for the panels with installed end face profile

Calculation of the average load value, the standard deviation of the unit load values, and the coefficient of variation were carried out similarly to chapter 3.1.

Delamination did not occur in both schemes of installation of the end face profile with an edge distance of 50 mm. The loss of bearing capacity was a result of the pull-out of a rivet.

Table 5. Results of pulling test for the samples with installed end face profile.

Installation scheme	$N_{average}$, kN	S, kN	v	F_n, kN
Coaxial	0.67	0.049	0.073	0.508
Span	0.639	0.072	0.112	0.433

3.3. Cyclic load action

The cyclic tests described in chapter 2.3 led to the results given in Table 6.

Table 6. Results of cyclic loading.

Sample number	Duration, s	Number of cycles	Loading speed, mm/min	Type of cycle	$F_{(-)}$, kN	$F_{(+)}$, kN	Δ, mm	$F_{destructive}$, kN
1	340	4	10	Non-uniform	-0.400	0.218	-	0
2	134	2	10	Non-uniform	-0.450	0.245	-	0.305
3	199	21	10	Non-uniform	-0.450	0.245	-	0.345
4	130	2	10	Non-uniform	-0.450	0.245	-	0.328
5	225	3	10	Non-uniform	-0.400	0.218	-	0.26
6	472	6	10	Non-uniform	-0.400	0.218	-	0.261
7	1747	21	11	Non-uniform	-0.350	0.191	-	0.264
8	4243	52	11	Non-uniform	-0.350	0.191	-	0.276
9	9708	131	11	Non-uniform	-0.300	0.164	-	0.06
10	**23993**	**550**	**11**	**Non-uniform**	**-0.158**	**0.086**	**0.44**	**no destruction**
11	**22293**	**365**	**11**	**Non-uniform**	**-0.250**	**0.136**	**0.92**	**no destruction**
12	9420	125	11	Uniform	-0.250	0.250	-	0.25
13	**28228**	**558**	**11**	**Uniform**	**-0.158**	**0.158**	**0.90**	**no destruction**
14	16090	229	11	Uniform	-0.250	0.250	-	0.25
15	**27179**	**462**	**11**	**Non-uniform**	**-0.250**	**0.136**	**0.73**	**no destruction**
16	**29264**	**542**	**11**	**Uniform**	**-0.158**	**0.158**	**0.55**	**no destruction**
17	**28178**	**485**	**11**	**Uniform**	**-0.158**	**0.158**	**0.85**	**no destruction**
18	**27640**	**520**	**11**	**Uniform**	**-0.158**	**0.158**	**0.83**	**no destruction**
19	**29647**	**550**	**11**	**Uniform**	**-0.158**	**0.158**	**0.77**	**no destruction**
20	**28331**	**581**	**11**	**Uniform**	**-0.158**	**0.158**	**0.72**	**no destruction**

Samples withstood more than 485 uniform cycles without visible fracture under the action of an alternating load equal to:

$$F_{\pm} = \pm 0.158 \text{kN}$$

Samples withstood more than 365 non-uniform cycles without visible fracture under the action of an alternating load equal to:

$$F_{+} = 0.136 \text{kN}; F_{-} = -0.25 \text{kN}$$

Subsequent pulling tests showed a presence of residual load bearing capacity.

Table 7. Results of pulling test for the samples after cyclic loading.

Sample number	$N_{critical}$, kN	$N_{average}$, kN	$(N_{critical} - N_{average})^2$, kN	S, kN	$N-3S$, kN	$N+3S$, kN	v	R_{n95}, kN
13	0.61		0.0023592					
15	0.48		0.0066306					
16	0.58		0.0003449					
17	0.56	0.561	2.041E-06	0.065	0.757	0.366	0.116	0.365
18	0.51		0.0026449					
19	0.52		0.0017163					
20	0.67		0.0117878					

Therefore, for calculation purposes F_+ and F_- can be assumed as values of pulling force in the connection between a blind rivet with a diameter of 4.8 mm and the outer sheet of the sandwich panel with the thickness of 0.5 mm for the angular zone of application of the peak wind load, when aerodynamic coefficients of such zone correspond to the values below:

$$F_+ = 0.136\text{kN}; F_- = -0.25\text{kN}; \frac{F_-}{F_+} = -1.83$$

if at least 10 samples were subjected to an experimental study with a similar test load.

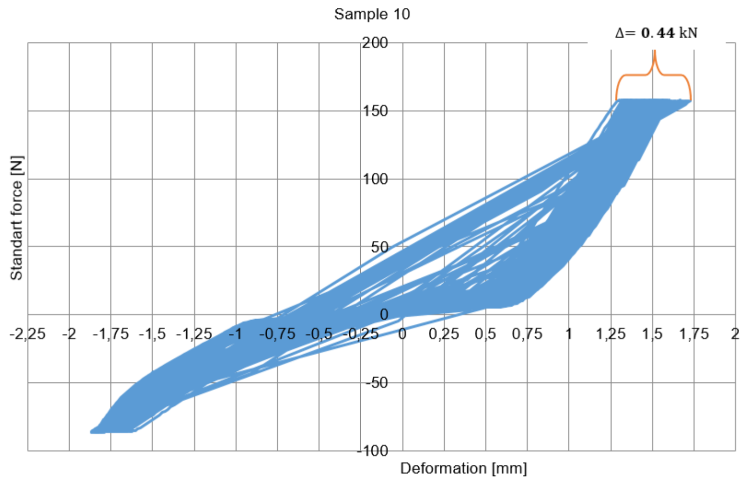

Figure 30. Cyclic load action on sample 10.

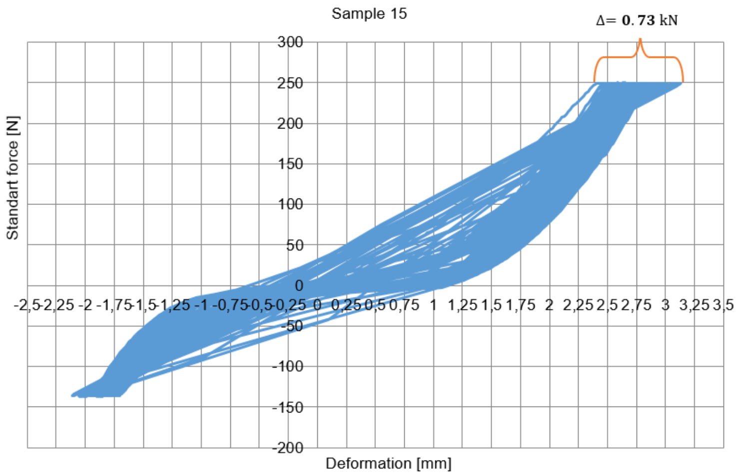

Figure 31. Cyclic load action on sample 15.

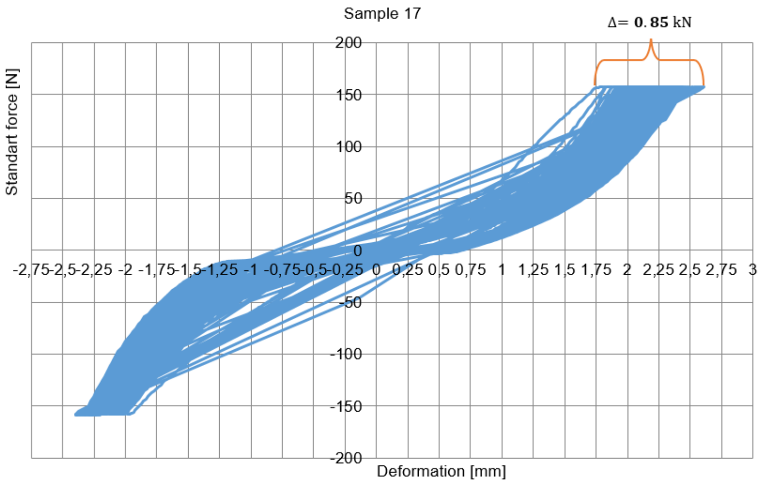

Figure 32. Cyclic load action on sample 17.

The values of bearing capacity of the connection obtained under cyclic loading, which imitates peak wind loads, are significantly lower than the values for a single pulling load. Therefore, existing practical methods of determination of the bearing capacity based solely on single loading should be improved and extended.

3.4. Pulling test for a group of rivets

Tests were performed in order to determine the bearing capacity of the fastening of the subframe to the sheathing of the sandwich panel by means of a group of blind rivets (chapter 2.4).

Test schemes were verified with the aim of preventing sandwich panel delamination.

• Schemes of the tests which ended by delamination of the samples:

First scheme option (Figure 24)

Maximum loads under the combined action of shear force and pulling force:

$$P_{hor} = const = 0.3\text{kN}; F_{\max} = 2.1\text{kN}$$

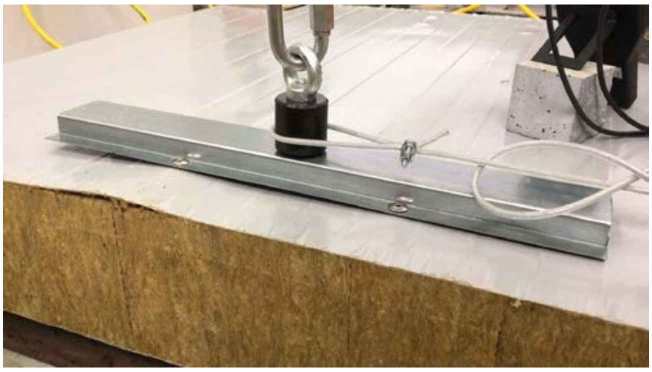

Figure 33. Delamination at $F_{\max} = 2.1\text{kN}$.

Maximum loads action of pulling force (without shear force):

$$P_{hor} = const = 0; F_{\max} = 1.7\text{kN}$$

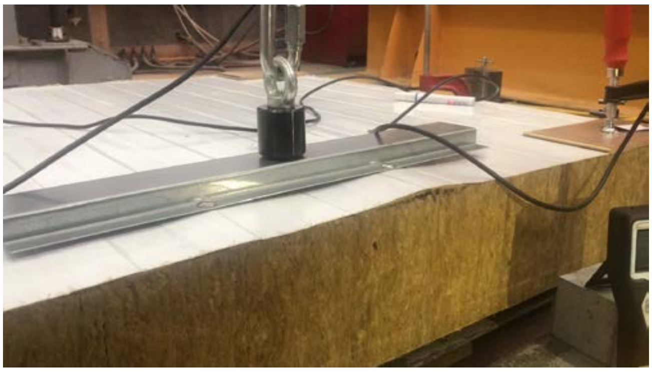

Figure 34. Delamination at $F_{\max} = 1.7\text{kN}$.

Second scheme option (Figure 25)

Maximum loads under the combined action of shear force and pulling force:

$$P_{hor} = const = 0.3\text{kN}; F_{\max} = 1.6\text{kN}$$

Third scheme option (Figure 26)

Maximum loads under the combined action of shear force and pulling force:

$$P_{hor} = const = 0.3\text{kN}; F_{\max} = 1.1\text{kN}$$

• Schemes of the tests which ended by pulling of the blind rivets:

Forth scheme option (coaxial) (Figure 27)

$$F_{max} = 1.3\text{kN}$$

Fifth scheme option (span) (Figure 28)

$$F_{max} = 1.9\text{kN}$$

Existing researches [3]–[5], [8], [11]–[13], [15] present studies on the phenomena of delamination and associated issues for sandwich panels with the type of a core other than mineral wool. Therefore, final results could not be comprehensively compared, however, the main approaches, methods, and general principles of calculation in accordance with Limit State design remain analogous.

4. Conclusions

The study was devoted to the investigation of the fastening to an outer steel sheet of a sandwich panel with mineral wool insulation core. The proposed test bench for the experimental investigation of the considered structural solution was described. For the studied type of panel following conclusions regarding the connection between the rivet and the outer sheet of the sandwich panel were made:

1. Edge distance equal to 75 mm or more does not affect the bearing capacity of the joint in considered structural solution.

2. Cyclic load action, which imitated peak wind loads on the panel, significantly reduced the bearing capacity of the connection in comparison with single pulling loading. It is recommended to assume the value of the bearing capacity of the connection based on the calculation made for the cyclic exposure corresponding to peak wind loads.

3. In systems where the fastening is made to an outer metal sheet when an end face profile is installed, the fastening element can be attached to the outer sheet of the sandwich panel with an edge distance of 50 mm if the step of placement of self-tapping fastening screws does not exceed 200 mm. Since the location of self-tapping screws from the position of the fastening elements affects the bearing capacity of the connection, it is recommended to install self-tapping screws at a distance of at least 75 mm from the connection.

4. Rivets used for fastening the subframe of the curtain wall system should be placed taking into account the position of the fastening element of cladding, from which concentrated load will be transferred to the system.

5. Recommended scheme of the attachment of the curtain wall subframe to the outer sheet of sandwich panels with a thickness of 0.5 mm is showed below:

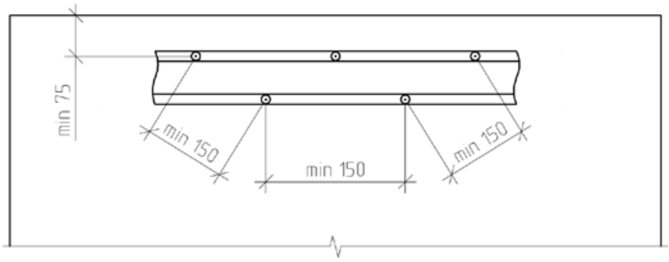

Figure 35. Recommended scheme of the attachment of the curtain wall subframe

References

1. Shazly, M., Bahei-El-Din, Y., Salem, S. Characterization of sandwich panels for indentation and impact. Journal of Physics: Conference Series. 2013. 451(1). DOI:10.1088/1742-6596/451/1/012001.
2. Paulson, S., Kedir, N., Sun, T., Fezzaa, K., Chen, W. Observation of Dynamic Adhesive Behavior Using High-Speed Phase Contrast Imaging. Proceedings of the Annual Conference on Experimental and Applied Mechanics. Reno, 2019. No. 1. Pp. 197–199. DOI: 10.1007/978-3-030-30021-0_34.
3. Cai, S., Liu, J., Zhang, P., Li, C., Cheng, Y. Dynamic response of sandwich panels with multi-layered aluminum foam/UHMWPE laminate cores under air blast loading. International Journal of Impact Engineering. 2020. No. 138. DOI: 10.1016/j.ijimpeng.2019.103475.
4. Studzinski, R., Pozorski, Z., Garstecki, A. Failure maps of sandwich panels with soft core. Proceedings of the 10th International Conference Modern Building Materials, Structures and Techniques. Vilnius, 2010. Pp. 1060–1065.
5. Mamalis, A.G., Spentzas, K.N., Manolakos, D.E., Ioannidis, M.B., Papapostolou, D.P. Experimental investigation of the collapse modes and the main crushing characteristics of composite sandwich panels subjected to flexural loading. International Journal of Crashworthiness. 2008. 13(4). Pp. 349–362. DOI: 10.1080/13588260801933691.
6. Mostafa, A., Shankar, K. In-plane shear damage prediction of composite sandwich panel with foam core. Applied Mechanics and Materials. 2013. No. 376. Pp. 69–73. DOI:10.4028/www.scientific.net/AMM.376.69.

7. Ma, J., Yan, Y. Multi-scale simulation of stitched foam-core sandwich composites subjected to low-velocity impact. Acta Metallurgica Sinica. 2013. 30(1). Pp. 230–235.
8. Rabeih, E.-A.M., Elghandour, E.I. Delamination detection inside composite structures plates under free vibration. Proceedings of the International SAMPE Technical Conference. Long Beach, California, 2013. Pp. 956–972.
9. Wang, J., Li, J., Gangarao, H., Liang, R., Chen, J. Low-velocity impact responses and CAI properties of synthetic foam sandwiches. Composite Structures. 2019. No. 220. Pp. 412–422. DOI:10.1016/j.compstruct.2019.04.045.
10. Ahmadi, H., Liaghat, G. Analytical and experimental investigation of high velocity impact on foam core sandwich panel. Polymer Composites. 2019. 40(6). Pp. 2258–2272. DOI:10.1002/pc.25034.
11. Odessa, I., Frostig, Y., Rabinovitch, O. Dynamic interfacial debonding in sandwich panels. Composites Part B: Engineering. 2020. No. 185. DOI:10.1016/j.compositesb.2019.107733.
12. Medina, S.A., Meza, J.M., Kawashita, L.F. Damage sequence of honeycomb sandwich panels under bending loading: Experimental and numerical investigation. Journal of Reinforced Plastics and Composites. 2020. 39(5–6). Pp. 175–192. DOI: 10.1177/0731684419880970.
13. Liu, J., Zhang, T., Jiang, W., Liu, J. Mechanical response of a novel composite Y-frame core sandwich panel under shear loading. Composite Structures. 2019. No. 224. DOI:10.1016/j.compstruct.2019.111064.
14. Aryal, B., Morozov, E. V, Wang, H., Shankar, K., Hazell, P.J., Escobedo-Diaz, J.P. Effects of impact energy, velocity, and impactor mass on the damage induced in composite laminates and sandwich panels. Composite Structures. 2019. No. 226. DOI:10.1016/j.compstruct.2019.111284.
15. Rejab, M.R.M., Bachtiar, D., Siregar, J.P., Paruka, P., Fadzullah, S.H.S.M., Zhang, B., Cantwell, W.J. The mechanical behavior of foam-filled corrugated core sandwich panels in lateral compression. Proceedings of the American Society for Composites 31st Technical Conference. Williamsburg, Virginia 2016.
16. Correia, J.R., Garrido, M., Gonilha, J.A., Branco, F.A., Reis, L.G. GFRP sandwich panels with PU foam and PP honeycomb cores for civil engineering structural applications: Effects of introducing strengthening ribs. International Journal of Structural Integrity. 2012. 3(2). Pp. 127–147. DOI:10.1108/17579861211235165.
17. Judawisastra, H., Ivens, J., Verpoest, I. The fatigue behaviour and damage development of 3D woven sandwich composites. Composite Structures. 1998. 43(1). Pp. 35–45. DOI: 10.1016/S0263-8223(98)00093-2.
18. Anoshkin, A.N., Zuiko, V.Y., Alikin, M.A., Tchugaynova, A. V. Influence of delamination on the mechanical properties of composite sandwich-panels. Proceeding of the 17th European Conference on Composite Materials. Munich, 2016.
19. Höwer, D., Jois, K.C., Lerch, B.A., Bednarcyk, B.A., Pineda, E.J., Reese, S., Simon, J.-W. Relevance of 3D simulations and sandwich core topology for the modeling of honeycomb core sandwich panels undergoing interfacial crack propagation. Composite Structures. 2018. No. 202. Pp. 660–674. DOI:10.1016/j.compstruct.2018.03.067.
20. Höwer, D., Jois, K.C., Bednarcyk, B.A., Pineda, E.J., Reese, S., Simon, J.-W. A novel mixed-mode cohesive zone model for delamination with severe fiber bridging applied to sandwich panels and monolithic laminates. Proceeding of the 18th European Conference on Composite Materials. Athens, 2018.
21. Ma, M., Yao, W., Chen, Y. Critical energy release rate for facesheet/core delamination of sandwich panels. Engineering Fracture Mechanics. 2018. No. 204. Pp. 361–368. DOI:10.1016/j.engfracmech.2018.10.029.
22. Ungermann, D., Lübke, S., Urbanek, D. Combined load bearing behaviour of face sheet and foam core of sandwich panels subjected to localised loads. Bauingenieur. 2013. No. 88. Pp. 261–268.

Information about authors

Alexander Galyamichev
ORCID: https://orcid.org/0000-0003-4992-2084
E-mail: gav@spbstu.ru

Ekaterina Gerasimova
ORCID: https://orcid.org/0000-0002-6056-5498
E-mail: katyageras17@gmail.com

Denis Egorov
ORCID: https://orcid.org/0000-0001-9282-3255
E-mail: egorov.dv@edu.spbstu.ru

Dmitrijs Serdjuks
Doctor of Technical Science
ORCID: https://orcid.org/0000-0002-1843-3061
E-mail: Dmitrijs.Serdjuks@rtu.lv

Anna Grossman
ORCID: https://orcid.org/0000-0003-4851-4687
E-mail: grosswoman96@gmail.com

Dmitry Lysenko
ORCID: https://orcid.org/0000-0001-5535-4701
E-mail: dmitry_0798@mail.ru

Received 08.10.2020. Approved after reviewing 19.12.2021. Accepted 19.01.2022.